FORMULAS FOR RADIANT HEAT TRANSFER BETWEEN NONGRAY PARALLEL PLATES OF POLISHED REFRACTORY METALS

by J. Robert Branstetter

Lewis Research Center

Cleveland, Ohio

FORMULAS FOR RADIANT HEAT TRANSFER BETWEEN NONGRAY

PARALLEL PLATES OF POLISHED REFRACTORY METALS

By J. Robert Branstetter

Lewis Research Center
Cleveland, Ohio

NATIONAL AERONAUTICS AND SPACE ADMINISTRATION

FORMULAS FOR RADIANT HEAT TRANSFER BETWEEN NONGRAY

PARALLEL PLATES OF POLISHED REFRACTORY METALS

by J. Robert Branstetter

Lewis Research Center

SUMMARY

Hemispherical emittance, both total and normal, were calculated from normal spectral-emittance data obtained from other sources. The metals evaluated were clean, polished tungsten, molybdenum, and tantalum, each of which exhibits spectral emittances that vary considerably with temperature and wavelength.

Net radiant heat flow between two parallel, infinite plates was computed by summing the monochromatic energy exchange. The evaluation was made for all nine possible combinations obtained by interchanging metals on the two surfaces. The results are graphically presented as a function of the temperatures of the two surfaces. Equations of the form

$$q = a\left(T_1^b - T_2^b\right)\left(\frac{T_2}{T_1}\right)^c$$

were fitted to each of the nine sets of heat-flux calculations, where q is the heat-transfer rate, and T_1 and T_2 are the temperatures of the hotter and cooler surfaces, respectively. Values of the constants, a, b, and c are presented along with contour plots showing the temperature regions in which the equations are accurate to 7 and 11 percent, respectively. These equations are shown to be more simple and considerably more accurate than conventional gray-body equations in representing machine-calculated nongray-body heat flux.

The computational procedures for obtaining the heat flux and the constants in the arbitrary equations are described.

INTRODUCTION

Advances in high-temperature technology during the last decade have resulted in many applications requiring refractory metals. These metals are finding uses in their pure form, in alloys, and in certain compounds such as carbides that exhibit many metallic characteristics. The spectral emittance of these materials is highly sensitive to

wavelength. For a spectrally selective material, the total emittance and total absorptance are not equal; hence the conventional gray-body heat-exchange equations based on the interchangeability of emittance and absorptance are invalid. The proper procedure is to sum the monochromatic energy exchange over all wavelengths of heat radiation. This summation method is used herein to evaluate the net heat exchange between two parallel, infinite surfaces of clean, polished tungsten, molybdenum, and tantalum. The evaluation was made with a digital computer for all nine possible combinations of hot and cold surfaces. Each surface was at a uniform temperature that was varied from about the melting point to almost 500° K. The results are presented in graphical form and in the form of fitted equations.

Hemispherical spectral and hemispherical total emittances, computed from the normal spectral-emittance data of reference 1, are also included. These data, which are for very pure, single crystal metals, are compared to results of other investigators.

ANALYSIS

The equation and a computational procedure for evaluating the nongray-body heat flux between the two parallel, infinite surfaces of opaque material are described in detail in references 2 and 3.

The basic method, most frequently called the summation method, incorporates the following assumptions or conditions:

(1) Each surface is at a constant temperature.

(2) Each surface is a diffuse radiator.

(3) At a given temperature and wavelength the hemispherical spectral absorptance equals the hemispherical spectral emittance.

(4) A vacuum exists between the two plates.

The nongray-body net heat flux q_{ng} in watts per square centimeter is given by

$$q_{ng} = \int_0^{\lambda=\infty} \frac{d\lambda}{\epsilon_{\lambda,T_1}^{-1} + \epsilon_{\lambda,T_2}^{-1} - 1} \left(J_{\lambda,T_1} - J_{\lambda,T_2} \right) \tag{1}$$

(symbols are defined in appendix A.) In the finite difference formed required by the machine calculators, the spectral emittance of wavelengths greater than 20 microns was assumed to be constant and the energy at wavelengths less than 0.2 micron was negligible. Equation (1) then becomes

2

$$q_{ng} = \left[\sum_{\lambda=0.2}^{\lambda=20} \frac{\Delta\lambda}{\epsilon_{\lambda,T_1}^{-1} + \epsilon_{\lambda,T_2}^{-1} - 1} \left(J_{\lambda,T_1} - J_{\lambda,T_2}\right) \right] + \frac{1}{\epsilon_{20,T_1}^{-1} + \epsilon_{20,T_2}^{-1} - 1}$$

$$\times \left[\left(\sigma T_1^4 - \sum_{\lambda=0.2}^{\lambda=20} J_{\lambda,T_1} \Delta\lambda\right) - \left(\sigma T_2^4 - \sum_{\lambda=0.2}^{\lambda=20} J_{\lambda,T_2} \Delta\lambda\right) \right] \qquad (2)$$

The flux per square centimeter emitted by a surface is $\sigma \epsilon_T T^4$, where ϵ_T, the hemispherical total emittance at a particular temperature, is given by

$$\epsilon_T = \frac{1}{\sigma T^4} \int_0^{\lambda=\infty} \epsilon_{\lambda,T} J_{\lambda,T} \, d\lambda \qquad (3)$$

In finite difference form, equation (3) becomes

$$\epsilon_T = \frac{1}{\sigma T^4} \left[\left(\sum_{\lambda=0.2}^{\lambda=20} J_{\lambda,T} \epsilon_{\lambda,T} \Delta\lambda\right) + \left(\sigma T^4 - \sum_{\lambda=0.2}^{\lambda=20} J_{\lambda,T} \Delta\lambda\right) \epsilon_{20,T} \right] \qquad (4)$$

The size of the increment $\Delta\lambda$ was chosen to be constant at 0.05 micron.

The hemispherical spectral-emittance data to be used in the foregoing equations were computed from experimental measurements of normal spectral emittance (ref. 1). These normal emittances are shown in table I (p. 4). For tungsten and tantalum, metal temperatures were 1370°, 1920°, and 2480° K. Molybdenum data were obtained only at the two lower temperature values. The procedure of preparing these data for heat-flux calculations is as follows:

First, the tabulated normal data were converted to hemispherical spectral emittances by using figure 1, which was obtained by the E. Schmidt and Eckert method detailed in reference 4. Next, the results were plotted in
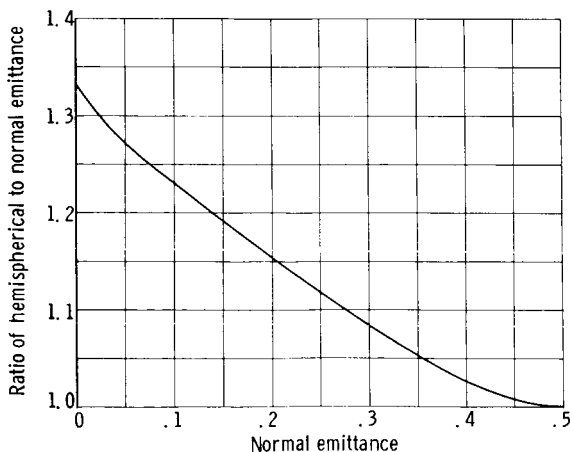

Figure 1. - Ratio of hemispherical to normal emittance of metallic surface.

3

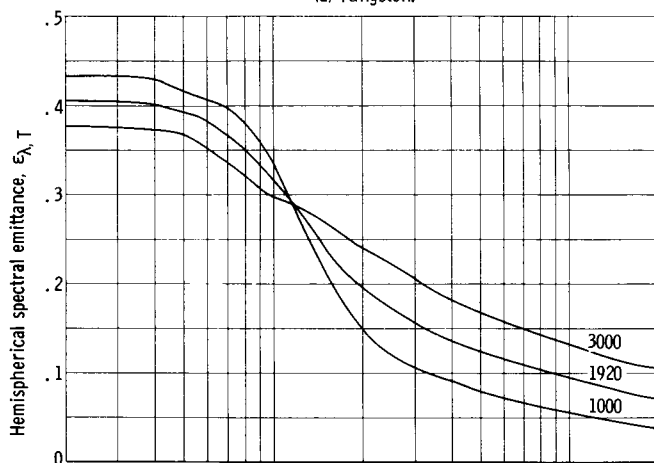TABLE I. - NORMAL SPECTRAL-EMITTANCE DATA OF

REFERENCE 1

Wavelength, λ, μ	Surface temperature, T, ^{O}K							
	1370	1920	2480	1370	1920	2480	1370	1920
	Normal spectral emittance, $\epsilon_{\lambda, T, n}$							
	Tungsten			Tantalum			Molybdenum	
0.42	0.478	0.463	0.456	0.520	0.511	0.502	0.406	0.388
.54	.462	.446	.438	.494	.471	.459	.392	.375
.68	.445	.428	.416	.426	.412	.407	.374	.353
1.00	.377	.365	.356	.255	.291	.312	.301	.289
1.28	.314	.309	.309	.196	.238	.267	.233	.240
1.60	.249	.257	.266	.167	.205	.236	.179	.197
2.00	.181	.204	.224	.149	.183	.210	.141	.167
2.50	.135	.164	.191	.136	.164	.189	.117	.145
3.00	.111	.140	.169	.126	.153	.178	.103	.130
4.00	.0879	.116	.143	.114	.137	.158	.0895	.113
5.00	.0763	.102	.127	.106	.126	.143	.0793	.102
6.00	.0693	.0945	.116	.098	.117	.133	.0716	.0956
7.00	.0642	.0866	.109	.0919	.110	.127	.0676	.0892
8.00	.0606	.0821	.104	.0884	.104	.120	.0647	.0840
9.00	.0568	.0779	.101	.0825	.0989	.116	.0589	.0798
10.00	.0547	.0753	.0969	.0795	.0949	.114	.0577	.0766
11.00	.0526	.0717	.0945	.0745	.0918	.109	.0561	.0739
12.00	.0475	.0669	.0877	.0736	.0870	.105	.0526	.0696
13.00	.0454	.0677	.0890	.0680	.0876	.103	.0511	.0687
14.00	.0463	.0658	.0847	.0734	.0839	.102	.0529	.0690
15.00	.0458	.0653	.0847	.0535	.0824	.105	.0442	.0636

a manner similar to that shown in figure 2(a), and extrapolated to wavelengths of 0.2 and 20 microns. Then at each wavelength to be used in the machine input, the data were plotted as emittance against temperature. Families of curves faired through the data points determined $\epsilon_{\lambda, T}$ at the values of temperature required by the calculation procedure. This technique presented a problem. The normal emittance of molybdenum had been evaluated at only two temperatures. This situation was handled by assuming molybdenum emittance possessed a nonlinear variation with temperature similar to that of tungsten and tantalum. As shown in appendix B, the procedure of preparing the $\epsilon_{\lambda, T, n}$ data provided room for only a small amount of "engineering error".

The machine data input were taken at the values of wavelength and temperature
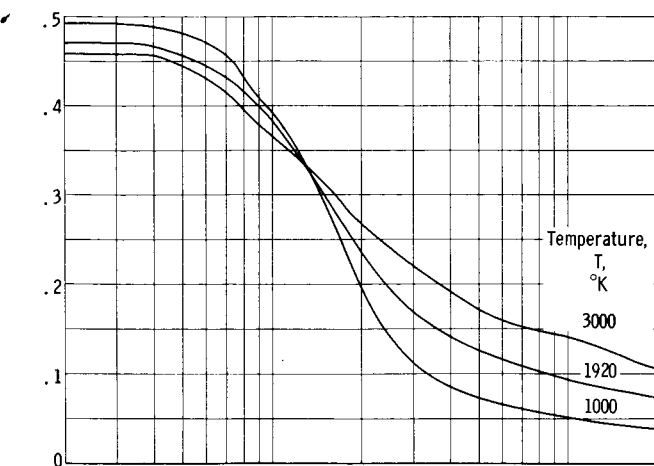
(a) Tungsten.

(b) Molybdenum.
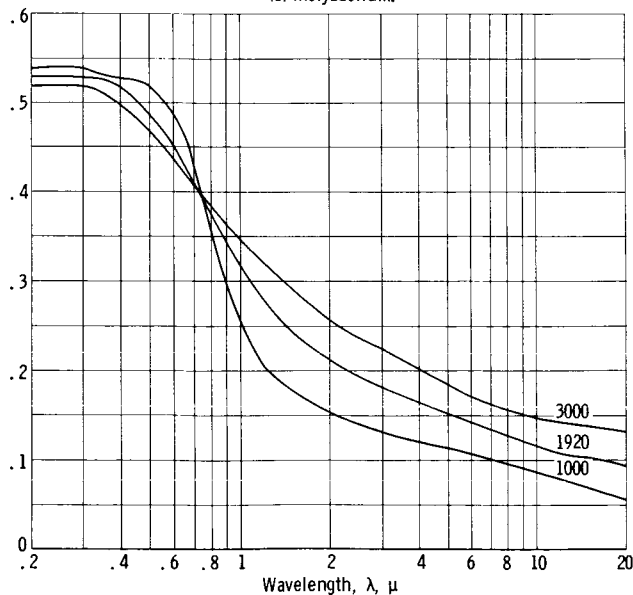
(c) Tantalum.

Figure 2. – Spectral-emittance data.
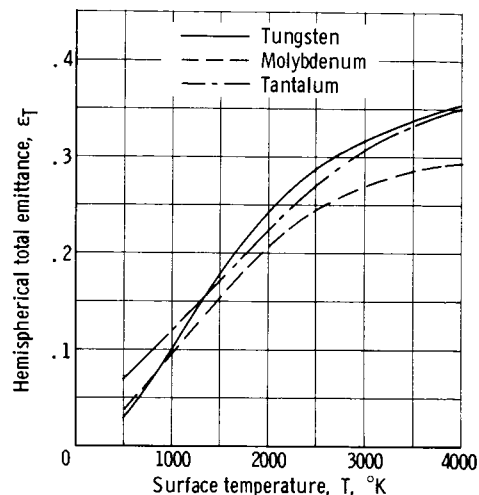
Figure 3. – Hemispherical total-emittance data.

listed in table II (p. 6). For any given temperature, a linear interpolation method was used to obtain $\epsilon_{\lambda, T}$ at all intermediate values of wavelength. Lagrangian interpolation or extrapolation was used to obtain $\epsilon_{\lambda, T}$ at the desired temperature.

RESULTS AND DISCUSSION

The calculated hemispherical spectral-emittance data for tungsten, molybdenum, and tantalum are presented in table II. These values are plotted in figure 2 for three of the five tabulated temperatures. Hemispherical total emittance results for the three metals are shown in figure 3.

The metal specimens for which the original data were obtained (ref. 1) were of high-purity monocrystalline structure. The surfaces had been polished either chemically or electrolytically to remove damaged

5

TABLE II. - HEMISPHERICAL SPECTRAL-EMITTANCE DATA

Surface temperature, T, °K

Hemispherical spectral emittance, $\epsilon_{\lambda, T}$

| Wavelength, λ, μ	Tungsten					Tantalum					Molybdenum				
	1000	1370	1920	2480	3000	1000	1370	1920	2480	3000	1000	1370	1920	2480	3000
0.2	0.492	0.482	0.470	0.462	0.458	0.539	0.535	0.528	0.523	0.519	0.434	0.423	0.406	0.3905	0.3774
.3	.492	.482	.470	.462	.458	.539	.535	.528	.523	.519	.434	.423	.406	.3905	.3774
.4	.489	.479	.467	.460	.456	.527	.523	.516	.507	.497	.430	.418	.401	.3860	.3734
.5	.480	.469	.455	.448	.445	.518	.505	.486	.475	.469	.417	.407	.3930	.3790	.3680
.6	.471	.459	.444	.435	.431	.485	.470	.452	.442	.438	.407	.3975	.3820	.3665	.3528
.7	.458	.446	.432	.421	.415	.434	.420	.412	.409	.408	.3970	.3850	.3665	.3500	.3360
.8	.432	.426	.417	.406	.3960	.3570	.3655	.3760	.3805	.3820	.3792	.3670	.3500	.3340	.3206
.9	.411	.406	.3990	.3890	.3786	.2964	.3190	.3440	.3565	.3636	.3580	.3470	.3325	.3185	.3064
1.0	.3908	.3875	.3815	.3735	.3650	.2550	.2838	.3170	.3374	.3470	.3338	.3260	.3150	.3050	.2970
1.1	.3728	.3690	.3635	.3580	.3538	.2284	.2582	.2962	.3200	.3336	.3036	.3010	.2985	.2950	.2940
1.25	.3437	.3415	.3375	.3370	.3364	.1990	.2310	.2714	.2990	.3154	.2634	.2680	.2750	.2800	.2830
1.4	.3145	.3145	.3145	.3175	.3204	.1852	.2132	.2530	.2826	.3002	.2326	.2405	.2530	.2640	.2740
1.6	.2726	.2782	.2860	.2940	.3018	.1706	.1966	.2355	.2660	.2852	.1970	.2090	.2277	.2455	.2612
1.8	.2300	.2415	.2590	.2725	.2826	.1596	.1852	.2228	.2522	.2700	.1702	.1855	.2090	.2305	.2490
2.0	.1968	.2112	.2345	.2545	.2684	.1528	.1772	.2134	.2408	.2562	.1510	.1686	.1967	.2200	.2396
2.2	.1690	.1885	.2160	.2390	.2560	.1486	.1712	.2046	.2306	.2476	.1344	.1550	.1855	.2125	.2332
2.5	.1415	.1622	.1935	.2216	.2412	.1410	.1634	.1935	.2195	.2364	.1216	.1422	.1730	.2000	.2212
3.0	.1136	.1359	.1677	.1987	.2200	.1320	.1522	.1818	.2078	.2256	.1058	.1264	.1568	.1840	.2050
3.5	.0985	.1205	.1520	.1830	.2042	.1260	.1445	.1730	.1965	.2134	.0976	.1170	.1450	.1710	.1910
4.0	.0868	.1090	.1410	.1705	.1912	.1208	.1390	.1645	.1865	.2020	.0918	.1105	.1375	.1625	.1826
5.0	.0750	.0950	.1255	.1530	.1716	.1146	.1300	.1520	.1710	.1845	.0804	.0980	.1250	.1495	.1698
6.0	.0672	.0870	.1160	.1415	.1600	.1068	.1205	.1420	.1600	.1722	.0728	.0900	.1165	.1410	.1612
8.0	.0590	.0760	.1025	.1280	.1492	.0958	.1085	.1280	.1455	.1584	.0648	.0810	.1040	.1255	.1432
10.0	.0520	.0685	.0935	.1195	.1408	.0866	.0990	.1170	.1355	.1480	.0564	.0730	.0955	.1165	.1338
12.0	.0464	.0625	.0870	.1125	.1340	.0798	.0905	.1080	.1300	.1438	.0516	.0665	.0880	.1075	.1236
16.0	.0416	.0570	.0795	.1000	.1170	.0665	.0800	.1020	.1225	.1384	.0444	.0580	.0775	.0960	.1106
20.0	.0398	.0545	.0740	.0925	.1056	.0570	.0705	.0925	.1150	.1328	.0390	.0525	.0725	.0910	.1060

material contained in the surface layers. The emittance measurements had been carried out in a high-vacuum environment and in accordance with good spectrographic practices. Crystal orientation was found to have little influence on emittance results. For each metal, the spectral emittance values were smaller than those of unpolished specimens of polycrystalline material (ref. 5). This effect was most noticeable at the longer wavelengths of radiation.

A comparison of the present emittance data with similar data from other sources would be of interest. Recent studies (ref. 6) by Parker and Abbott on clean specular surfaces of polycrystalline tungsten and tantalum have yielded ϵ_T data at temperatures of 1100° to 3000° K. These data can be compared directly to the data shown in figure 3 (p. 5). At temperatures above 1400° K, the agreement was excellent; however, as the temperature was decreased from 1400° to 1100° K, Parker and Abbott reported progressively smaller emittances than those presented herein. This effect was approximately twice as great for tantalum as for tungsten. Maximum observed discrepancies were approximately 8 percent.

The nongray-body heat-transfer data for the three metals are presented in figure 4. Net heat transfer is plotted as a function of $T_1 - T_2$ with T_1 as the parameter. The heavy solid lines show the region encompassed by the smoothed data from reference 1. The lighter solid lines show the calculations based on the temperature extrapolations previously described. The dashed lines are the values beyond the temperatures of the machine calculations and are simply faired-in curves of heat transfer as a function of $T_1 - T_2$. It is well to note that rather large heat-flux errors could accrue from extrapolation of the $\epsilon_{\lambda, T}$ data to the lower temperatures shown in figure 4.

All data curves of figure 4 exhibit a maximum in the value of q_{ng}. This maximum is most noticeable under the combined effect of large T_1 and a tantalum cold surface (figs 4(c), (f), and (i)). One contributing factor is the extent the absorptance of the colder surface decreases with decreasing temperature. At wavelengths near 1 micron (where an appreciable amount of blackbody radiation occurs at high temperature levels), only tantalum exhibits a decrease in spectral absorptance as the temperature is lowered (see fig. 2, p. 5).

The assumption that the surfaces radiate diffusely can lead to error in the values of q_{ng}. An alternate method (ref. 7) of calculating q_{ng} assumes the energy exchange is entirely specular and that the angular distribution of energy is defined by the Fresnel equations. Exploratory calculations indicate that this alternate method would yield q_{ng} values 3 to 5 percent greater than those presented herein. Since the radiant energy exchange between real surfaces is neither entirely specular nor entirely diffuse, it is fortunate that the two limiting situations yield such good agreement in the value of net heat flux.
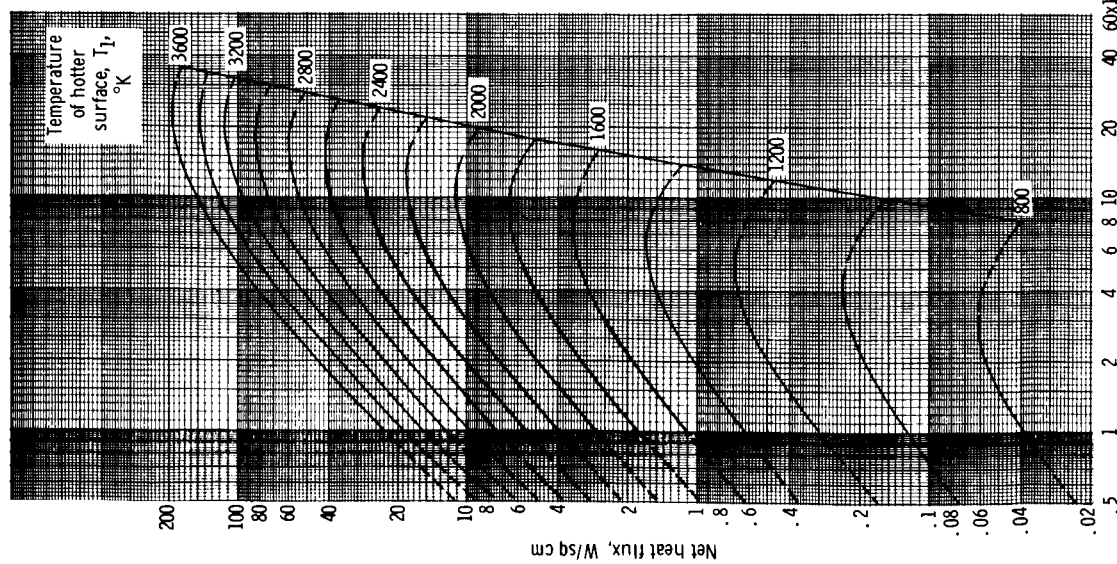
(a) Hotter surface, tungsten; colder surface, tungsten.
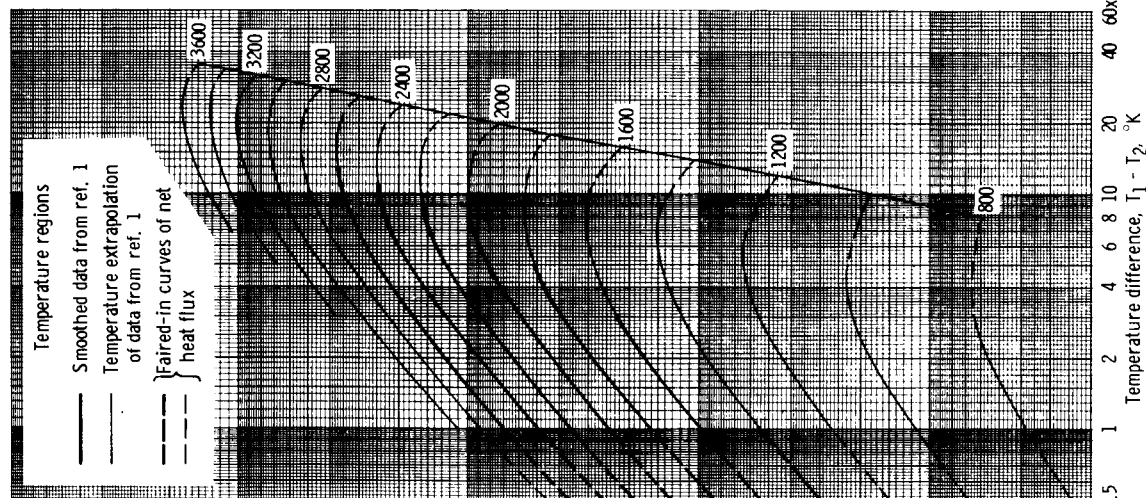
(b) Hotter surface, tungsten, colder surface, molybdenum.
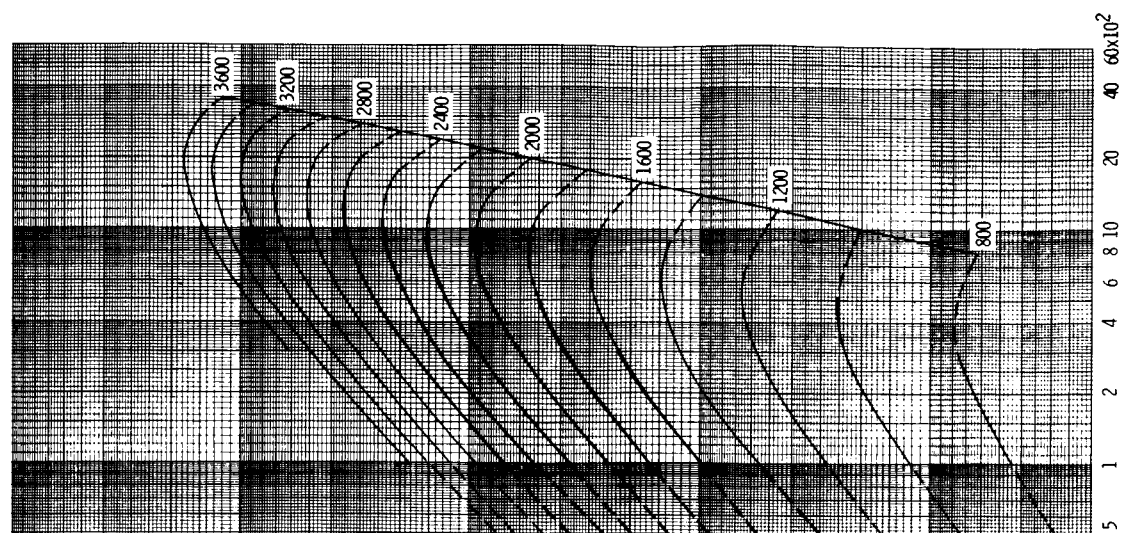
(c) Hotter surface, tungsten; colder surface, tantalum.

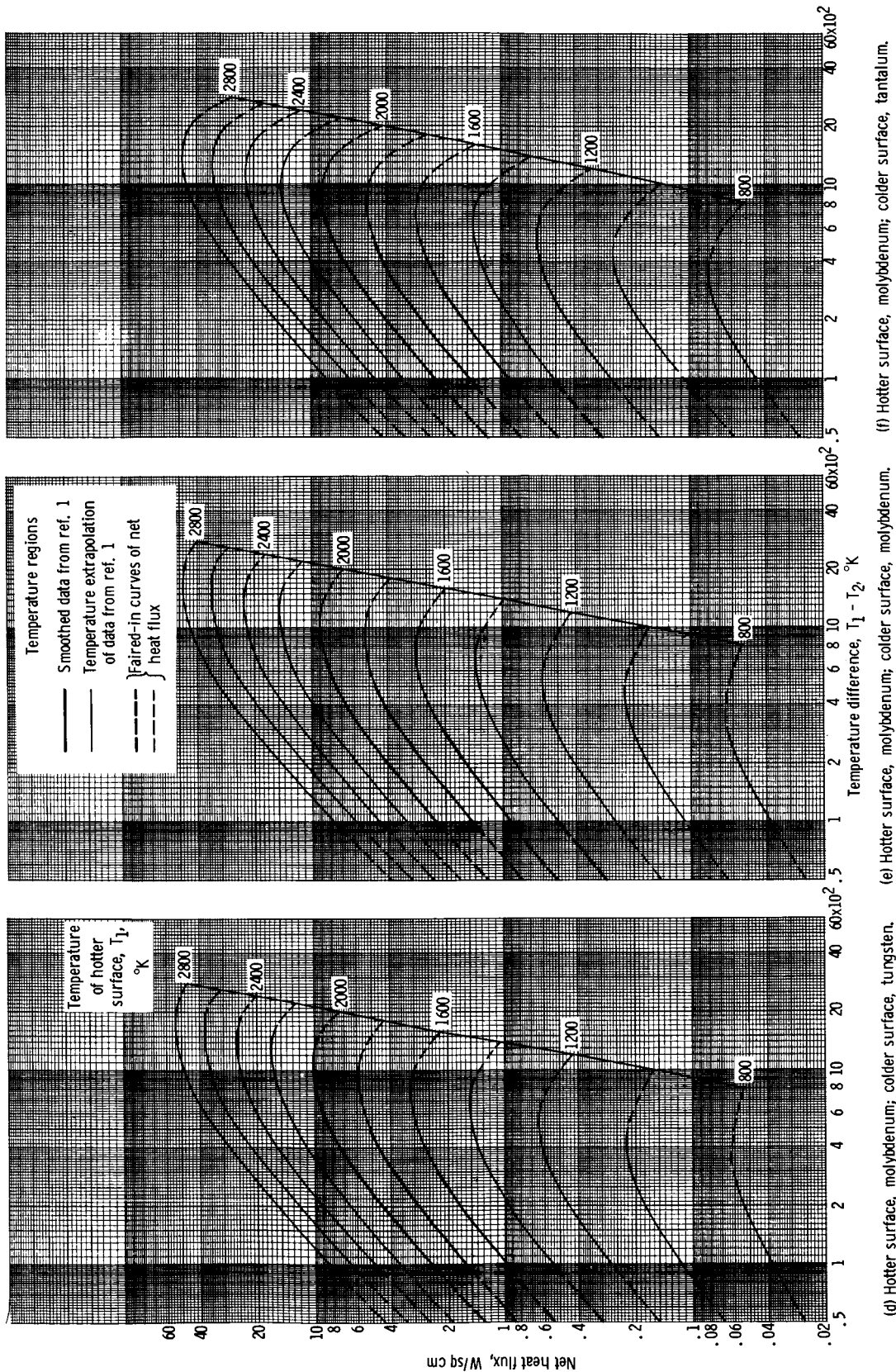Figure 4. - Net radiant heat flux between two infinite, parallel plates.

8

(d) Hotter surface, molybdenum; colder surface, tungsten.

(e) Hotter surface, molybdenum; colder surface, molybdenum.

(f) Hotter surface, molybdenum; colder surface, tantalum.

Figure 4. - Continued.

9

(g) Hotter surface, tantalum; colder surface, tungsten.

(h) Hotter surface, tantalum; colder surface, molybdenum.

(i) Hotter surface, tantalum; colder surface, tantalum.

Figure 4. - Concluded.

(a) Hotter surface, tungsten; colder surface, tungsten.

(b) Hotter surface, tungsten; colder surface, tantalum.
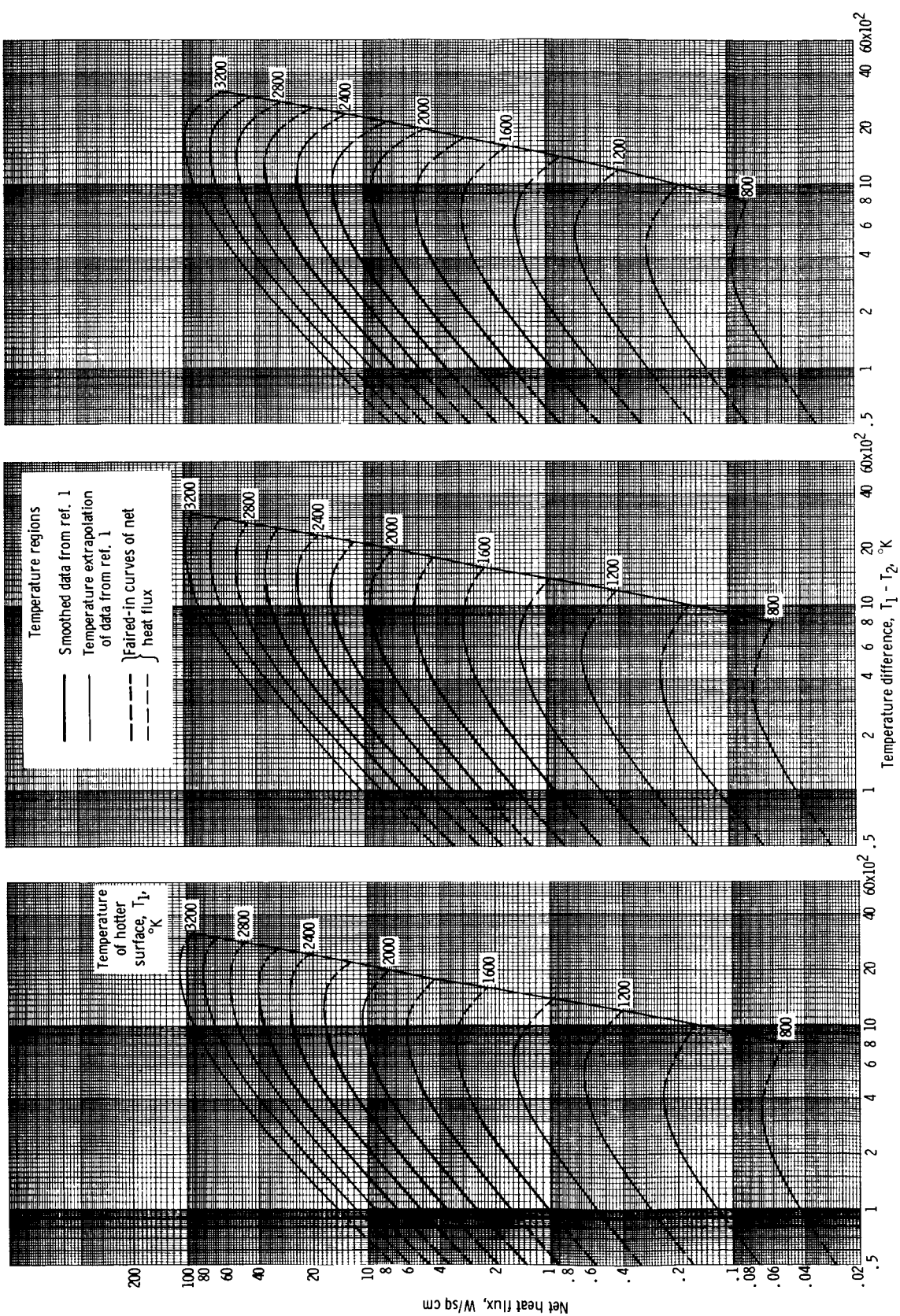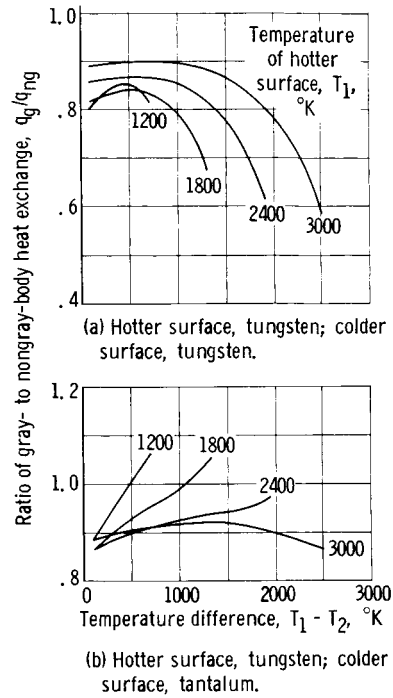
Figure 5. – Comparison of gray- and nongray-body methods for computing net heat flux between two infinite, parallel plates.

TABLE III. - CONSTANTS OF FORCE-FIT EQUATION (EQ. (6))

$$q_{ff} = a\left(T_1^b - T_2^b\right)\left(\frac{T_2}{T_1}\right)^c$$

Hotter surface, T_1	Cooler surface, T_2	Constant			Temperature of hotter surface, T_1, $^\circ K$	Equation (fig. 6)
		a	b	c		
Tungsten	Tungsten	0.353×10^{-15}	5.0	0	<3000	a
	Tungsten	$.166 \times 10^{-14}$	4.8	0	>2000	b
	Molybdenum	$.314 \times 10^{-15}$	5.0	0	<3000	c
	Molybdenum	$.149 \times 10^{-14}$	4.8	0	>2000	d
	Tantalum	$.335 \times 10^{-15}$	5.0	.17	------	e
Molybdenum	Tungsten	0.316×10^{-15}	5.0	0	------	f
	Molybdenum	.286	5.0	0	------	g
	Tantalum	.308	5.0	.17	------	h
Tantalum	Tungsten	0.328×10^{-15}	5.0	0	------	i
	Molybdenum	.294	5.0	0	------	j
	Tantalum	.326	5.0	.17	------	k

11

SIMPLE EQUATIONS FOR NET HEAT EXCHANGE

Simple expressions for net heat flux ease the mathematical complexity of analytical investigations. Two general types of equations were examined; namely, those based on conventional gray-body heat flow and those that express the net heat flux as an explicit function of T_1 and T_2.

The conventional gray-body net heat-transfer equation for closely spaced surfaces is

$$q_g = \sigma \frac{T_1^4 - T_2^4}{\epsilon_{T_1}^{-1} + \epsilon_{T_2}^{-1} - 1} \tag{5}$$

For this equation to be correct, the total emittance of a surface must equal its total absorptance. Since the refractory metals do not adhere to this restriction, discrepancies between the results of this equation and equation (1) are very large. The correlation can be improved by an empirical method (ref. 8, p. 63), which replaces ϵ_{T_2} in equation (5) by an effective emittance of the colder surface ϵ_{T*} evaluated at the geometric mean temperature

$$T^* = \sqrt{T_1 \times T_2}$$

The inaccuracy of this empirical equation is illustrated in figure 5(a), which is typical of those cases wherein tungsten or molybdenum was assigned to the colder surface. The nongray-body flux is larger than the gray-body flux and, in general, the error increases as T_1 is decreased and/or as ΔT is increased. Where tantalum was the colder surface, typical results are shown in figure 5(b).

Expressions that would possibly provide better correlations than those demonstrated in figure 5 were examined. Of the several expressions investigated, the "force-fit" equation

$$q_{ff} = a\left(T_1^b - T_2^b\right)\left(\frac{T_2}{T_1}\right)^c \tag{6}$$

yielded flux values most closely matching the values of equation (1). The constants a, b, and c for each set of metal surfaces were arrived at in the following manner: After assigning c a value of zero, a best value for b was determined. This was

12

-accomplished by fixing b at each of a number of set values between 4 and 6, and then solving for a while ranging the variables T_1 and T_2. The best value of b was the one that produced a minimum deviation in the value of a.   With b known, a best value for the constant c was determined in a manner similar to the determination of b.   Values of c smaller than 0. 1 had little influence and therefore were assigned a value of zero. Finally, with the constants b and c established, the constant a was picked such that a close fit would be obtained over the widest useable range of temperatures.

There exists an unlimited number of procedures for selecting the constants.   The procedure just described is better than some and is easily prepared for use in machine calculators.   The results are presented in table III (p. 11), and contour plots illustrating equation accuracy are shown in figure 6.   When constants were being fitted to equation (6), difficulties occurred in obtaining a reasonably satisfactory fit for several cases
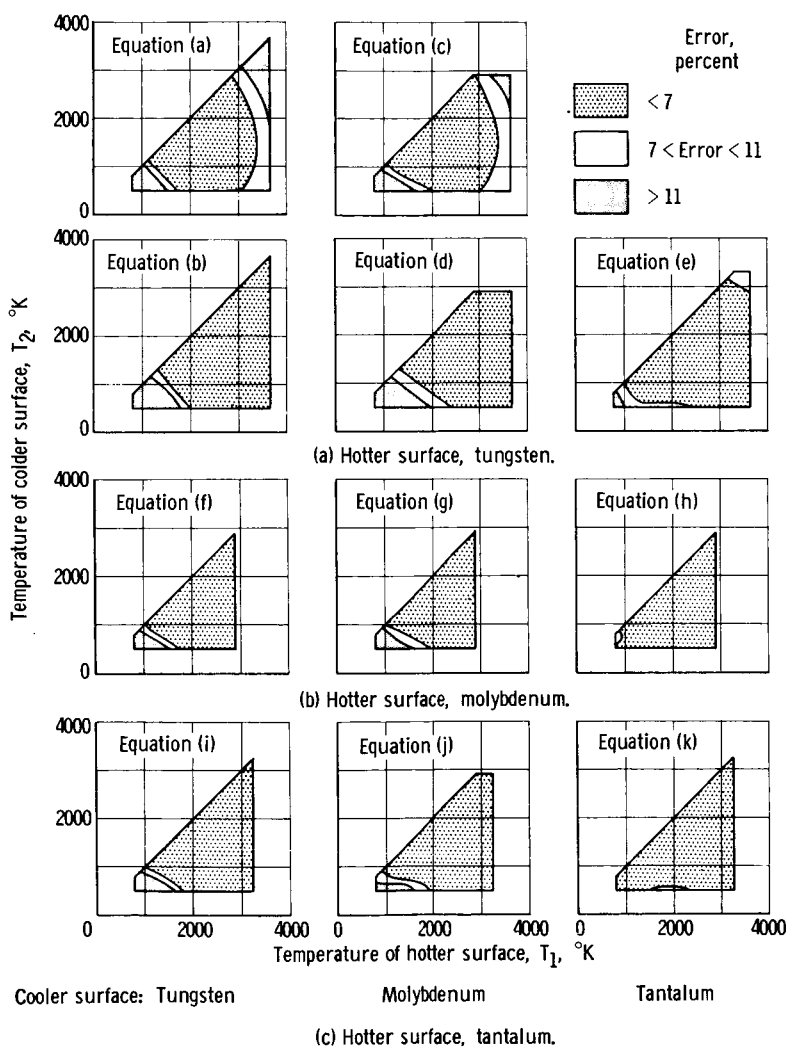

(a) Hotter surface, tungsten.

(b) Hotter surface, molybdenum.

(c) Hotter surface, tantalum.

Figure 6. – Error incurred with use of force-fit equations from table III. (Error is measured in percent deviation of net heat flux obtained by force fit from net heat flux obtained by summation.)

13

in which tungsten was the hotter surface. In each of these situations, two sets of constants are presented.

The values of flux given by the force-fit equation were larger than the nongray-body values in the low temperature region. No attempt was made to improve the fit because of the lack of low-temperature emittance data and hence the possible inaccuracy of the nongray-body heat-flux data.

Comparison of figures 5 and 6 shows that the force-fit equations more accurately represent the results of nongray-body heat-transfer calculations than the empirical gray-body equations. Also, within the larger shaded regions of figure 6 (where the error is less than 7 percent), it is very likely that the q_{ff} calculations are as accurate a measure of net heat flux as can be achieved in practice for real surfaces in a parallel-plate geometry.

The results of table III taken as a whole, show that the net heat exchange between two parallel, infinite surfaces of typical refractory metals is closely proportional to the fifth power of temperature throughout the temperature range investigated. The temperature-ratio factor is significant only for those cases in which tantalum is the cooler surface.

RÉSUMÉ

Hemispherical emittance, both total and normal, were calculated from normal spectral-emittance data obtained from other sources. The metals evaluated were clean, polished tungsten, molybdenum, and tantalum. Net radiant heat flow between two closely spaced plates was computed by summing the monochromatic energy exchange. This evaluation was made for all nine possible combinations obtained by interchanging metals on the two surfaces.

Simple equations were "force-fit" to the results of the heat-flux calculations. Reasonably good fits were established for a wide range of temperatures. The force-fit equations show much better agreement with machine-calculated heat fluxes than conventional gray-body equations, and are also easier to use.

Lewis Research Center,
    National Aeronautics and Space Administration
        Cleveland, Ohio, March 17, 1965.

APPENDIX A

SYMBOLS

a, b, c   constants

$J_{\lambda, T}$ Planck's distribution function,

$$37\ 404\lambda^{-5}\left(e^{14\ 387/\lambda T} - 1\right)^{-1},$$

$W/(\mu)(sq\ cm)$

q   heat-transfer rate

q_{ff} net heat-transfer rate for "force-fit" equation, $W/sq\ cm$

q_g net heat-transfer rate for gray-body conditions, $W/sq\ cm$

q_{ng} net heat-transfer rate for nongray-body conditions, $W/sq\ cm$

T   surface temperature, $^\circ K$

T^* $\sqrt{T_1 \times T_2}$

ϵ_T hemispherical total emittance

$\epsilon_{\lambda, T}$ hemispherical spectral emittance

$\epsilon_{\lambda, T, n}$ normal spectral emittance

λ wavelength, μ

σ Stefan-Boltzmann constant, $5.6699 \times 10^{-12}\ W/(sq\ cm)(^\circ K^4)$

Subscripts:

1   hotter surface

2   cooler surface

APPENDIX B

EXTRAPOLATION OF EMITTANCE DATA

Equations (1) and (2) require the emittance be independent of emission angle, that is, each surface emits according to the cosine law of Lambert. Therefore the normal emittance data of table I had to be converted to hemispherical values, $\epsilon_{\lambda, T}$. For diffuse radiators, a one to one relation exists. For polished metal surfaces, the hemispherical emittance can be obtained by means of figure 1. This conversion curve is based on equations (4-79), (4-84), and (4-85) of reference 4 relating electrical resistivity to emittance. The equations of little utility at the shorter wavelengths, appear satisfactory at wavelengths greater than 4 microns for smooth tungsten surfaces (ref. 2 and fig. 22, ch. 13 of ref. 9). A comparison of figures 1 and 2 shows the ratio $\epsilon_{\lambda, T}/\epsilon_{\lambda, T, n}$ to be largest in the region of greatest reliability of the equation. Hence, for polished surfaces, the conversion curve provides a fairly reliable means of obtaining heat-transfer results based on normal spectral-emittance data.

The aforementioned equations of reference 4 were used as guidelines to extrapolate the hemispherical-emittance data to wavelengths beyond 15 microns and to conduct temperature extrapolation of the emittance data at wavelengths greater than 4 microns.

Since very little energy is transferred at wavelengths less than 0.42 micron, a simple extrapolation, based on data of Larrabee (ref. 10) was used to extend the hemispherical emittances to a wavelength of 0.2 micron. Temperature extrapolation at short wavelengths was based on observations (ref. 9 and elsewhere) that for temperatures at least as small as 300° K, the emittance data for refractory metals pass through an inflection point (fig. 2).

REFERENCES

1. Dreshfield, R. L.; and House, R. D.: Investigation of the Spectral Normal Emittance of Single Crystals at High Temperatures. Rept. No. PWA-2306, Pratt & Whitney Aircraft, Feb. 15, 1964.

2. Branstetter, J. Robert: Radiant Heat Transfer Between Nongray Parallel Plates of Tungsten. NASA TN D-1088, 1961.

3. Branstetter, J. R.: Spectral Emissivities of Electrode Materials. Advanced Energy Conversion, vol. 3, no. 1, Jan.-Mar. 1963, pp. 295-303.

4. Jakob, Max: Heat Transfer. Vol. 1. John Wiley & Sons, Inc., 1949.

5. Anon.: Measurement of Spectral and Total Emittance of Materials and Surfaces Under Simulated Space Conditions. Rept. No. PWA-1863, Pratt & Whitney Aircraft, 1960.

6. Parker, W. J.; and Abbott, G. L.: Total Emittance of Metals. Symposium on Thermal Radiation of Solids, San Francisco, Calif., Mar. 4-6, 1964, Univ. Calif. Press, 1964.

7. Dunkle, R. V.: Emissivity and Inter-Reflection Relationships for Infinite Parallel Specular Surfaces. Symposium on Thermal Radiation of Solids, San Francisco, Calif., Mar. 4-6, 1964, Univ. Calif. Press, 1964.

8. McAdams, W. K.: Heat Transmission. Third ed., McGraw-Hill Book Co., Inc., 1954.

9. Worthing, Archie Garfield; and Halliday, David: Heat. John Wiley & Sons, Inc., New York, 1948.

10. Larrabee, Robert Dean: The Spectral Emissivity and Optical Properties of Tungsten. Tech. Rept. 328, Research Lab. of Electronics M.I.T., May 21, 1957. AD 156602.